

# Photothermal-assisted antibacterial application of GO-Ag against clinical isolated MDR *E. coli*

**Yuqing Chen**

The Affiliated Wuxi Maternity and Child Health Care Hospital of Nanjing Medical University

**Wei Wu**

The Affiliated Wuxi No. 2 People's Hospital of Nanjing Medical University

**Zeqiao Xu**

The Affiliated Wuxi People's Hospital of Nanjing Medical University

**Cheng Jiang**

The Affiliated Wuxi People's Hospital of Nanjing Medical University

**Shuang Han**

Jiangnan University

**Jun Ruan**

The Affiliated Wuxi People's Hospital of Nanjing Medical University

**Yong Wang** (✉ [wy8486@sina.com](mailto:wy8486@sina.com))

The Affiliated Wuxi People's Hospital of Nanjing Medical University of <https://orcid.org/0000-0002-4244-852X>

---

## Research

**Keywords:** In-vitro, MDR *E. coli*, graphene oxide-silver, photothermal treatment

**Posted Date:** November 7th, 2019

**DOI:** <https://doi.org/10.21203/rs.2.17020/v1>

**License:**  This work is licensed under a Creative Commons Attribution 4.0 International License.

[Read Full License](#)

---

# Abstract

**Background:** Treatment of multidrug-resistant (MDR) bacterial infection is a great challenge in public health. Herein, we provide a solution to this problem with the use of graphene oxide-silver (GO-Ag) nanocomposites as anti-bacterial agent.

**Methods:** Following established protocols, silver nanoparticles were grown on graphene oxide sheets. Then, a series of in-vitro studies were conducted to validate the antibacterial efficiency of the GO-Ag nanocomposites against clinical MDR *Escherichia coli* (*E. coli*) strains. Firstly, minimum inhibitory concentrations (MICs) of different antimicrobials were tested against MDR *E. coli* strains. Then, bacteria viability assessments were conducted with different nanomaterials in Luria-Bertani (LB) broth. Afterwards, photothermal irradiation was conducted on MDR *E. coli* with lower GO-Ag concentration. At last, fluorescent imaging and morphology characterization using scanning electron microscope (SEM) were done to find the possible cause of antibacterial effect.

**Results:** GO-Ag nanocomposites showed the highest antibacterial efficiency among tested antimicrobials. Synergetic antibacterial effect was observed in GO-Ag nanocomposites treated group. The remained bacteria viabilities were 4.4% and 4.1% respectively for different bacteria strains with GO-Ag concentration at  $14.0 \mu\text{g mL}^{-1}$ . In addition, GO-Ag nanocomposites have strong absorption in the near-infrared field and can convert the electromagnetic energy to heat. With the use of this photothermal effect, effective sterilization could be achieved using GO-Ag nanocomposites concentration as low as  $7.0 \mu\text{g mL}^{-1}$ . Fluorescent imaging and morphology characterization were used to analyze bacteria living status, which uncovered that bacteria integrity was disrupted after GO-Ag nanocomposites treatment.

**Conclusions:** GO-Ag nanocomposites are proved to be efficient antibacterial agent against multi-drug resistant *E. coli*. Their strong antibacterial effect arises from inherent antibacterial property and photothermal effect that provides aid for bacteria killing.

## Background

Antibiotics have been widely used for over 70 years in different fields such as medicines, agriculture and environment [1]. However, bacteria have developed resistance to antibiotics through acquired resistance genes or intrinsic antibiotic resistance capability [2], which leads to the wide existence of resistant bacteria, including multidrug-resistant (MDR) bacteria, extensively drug-resistant (XDR) bacteria and pandrug-resistant (PDR) bacteria [3]. In diagnosis practice, antibiotic resistance is a nonnegligible concern for clinical physicians to treat infections such as postoperative infections, ear, nose and throat (ENT) infections, and urinary tract infections. Antibiotic resistance makes antibiotic selection a great challenge as more and more MDR bacteria were found in patients [4–6]. Among all the infections encountered in hospital, urinary tract infections is one of the most common infections, in which case *E. coli* is found to be the major cause [7]. Moreover, spreading of certain type of antibiotics resistant *E. coli* may become potential cause for epidemic disease [8]. Several scientific reports have indicated that

antibiotic resistant *E. coli* bacteria are found in soil, water, foods and animals [9–15]. Due to the wide spread of antibiotic resistance bacteria and less efficiency of conventional antibiotics, alternatives are needed to deal with antibiotic-resistant bacteria.

Nanotechnology offers a new way to overcome healthcare challenges bring by antibiotic resistance bacteria, as the nanoscale antimicrobial agents has huge surface to volume ratio, and the size is comparable to the pathogenic microbes, allowing it penetrate into or contact with pathogenic microbes in efficient way [16]. Most of effective antimicrobials are metallic-based nanomaterials such as ZnO, TiO<sub>2</sub>, silver and gold nanoparticles [17–20]. Among different nanomaterials, silver-based nanomaterials are the most popular antibacterial agent [21, 22]. Silver nanoparticles (AgNPs) are effective against Gram-negative bacteria, Gram-positive bacteria, as well as MDR bacteria, while the antibacterial mechanism is still not clear though several hypotheses were propounded [23–26]. Graphene, a single layer of carbon atoms nanomaterial, has a unique set of physical, chemical and electronic properties [27–29], which enable it as novel agents for biomedical applications. Graphene-based nanomaterials are used as novel antimicrobial agents against broad-spectrum microbes via physical destruction of cell membrane and chemical damage bring by reactive oxygen species [30, 31]. However, there are debates on antibacterial activity of graphene and graphene oxide as several papers claimed little antibacterial activity of graphene oxide [32, 33]. Furthermore, graphene can be served as carrier for antibiotics delivery [34], and photothermal sensitizers in combination with near-infrared laser light for powerful photothermal killing of bacteria [35, 36].

GO-Ag nanocomposites are widely reported to be efficient antimicrobial agent to different kinds of microbes, including standard bacteria, fungus, resistance bacteria [37–42]. It shows better antibacterial efficiency in comparison with silver nanoparticles, because GO sheet provides anchor platform to make AgNPs well dispersed and large contact surface between bacteria and AgNPs [40, 43]. However, most of the studied bacteria were model bacteria instead of clinical isolated bacteria, especially MDR bacteria encountered in clinical practice. Furthermore, photothermal property of GO can be utilized for combined therapy to improve antibacterial efficiency, as well as to reduce risk of potential anti-nanomaterial resistance as silver resistance bacteria were reported [44, 45].

In order to find a way to address resistance problem of MDR bacteria encountered in clinical practice, photothermal-assistant anti-MDR *E. coli* bacteria study is conducted using synthesized GO-Ag nanocomposites. To achieve reliable antibacterial efficiency, we break study into 4 steps. 1<sup>st</sup> step is to verify the existence of synergistic effect of GO-Ag nanocomposite in comparison with AgNPs. MIC of AgNPs, GO-Ag, and some antibiotics are utilized to evaluate the antibacterial efficiency according to standard protocol. 2<sup>nd</sup> step is to find possible cause for improved antibacterial efficiency of GO-Ag, and to clarify the debates on GO antibacterial activity. Antibacterial efficiency of GO, AgNPs, GO-Ag, mixture of GO and AgNPs are studied simultaneously using MTT assay. In the 3<sup>rd</sup> step, *in vitro* photothermal-assistant treatment of MDR bacteria is conducted with energy from near-infrared laser light to kill MDR bacteria in more efficient way. Finally, characterization of GO-Ag treated bacteria is performed using confocal microscopy and SEM to indicate resulting damage after treatment.

## Methods

### Chemicals

AgNO<sub>3</sub>, sodium citrate, expandable graphite flakes, sodium chloride, H<sub>2</sub>SO<sub>4</sub>, KMnO<sub>4</sub>, 30% H<sub>2</sub>O<sub>2</sub>, HCl, NaOH are chemicals used for nanomaterials synthesis. Antibiotics including ampicillin, tetracycline, streptomycin, chloramphenicol are used for MIC testing. Tryptone, yeast extract, agar, dimethyl sulfoxide (DMSO), thiazolyl blue tetrazolium bromide (MTT) are used for bacteria culture and cell viability assay. All the reagents are purchased from Sigma-Aldrich.

### Bacteria Strain

2 MDR *E. coli* strains are isolated from urine samples in clinical lab. These two bacteria are named MDR-1 and MDR-2 respectively, and their antibiotic susceptibility were tested in clinical lab. MDR-1 is resistant to penicillin (ampicillin, AMP), tetracycline (tetracycline, TET), quinolone (nalidixic acid, NAL), and aminoglycoside (streptomycin, STR). MDR-2 is resistant to penicillin (ampicillin, AMP), tetracycline (tetracycline, TET), quinolone (nalidixic acid, NAL), aminoglycosides (spectinomycin, SPE; gentamicin, GEN), chloramphenicol (chloramphenicol, CHL).

### Preparation and characterization of GO, AgNPs and GO-Ag

AgNPs were synthesized according to previous reported method [46]. 18 mg silver nitrate was added into 100 mL distilled (DI) water, and the solution was heated in oil bath until boiling. Afterwards, 20 mg sodium citrate in 2 mL DI water were added to boiled silver nitrate solution slowly. Then solution was kept boiling for 1 hour. Cooling down the synthesized AgNPs solution at room temperature and took some sample for following characterization. Graphene oxide sheets were prepared using a modified Hummer method [47, 48]. Silver nanoparticles were deposited on GO sheets by using sodium citrate to reduce silver nitrate in GO aqueous solution. Briefly, 6 mg GO and 18 mg AgNO<sub>3</sub> were dissolved in 100 mL DI water under stirring in oil bath, and the solution was brought to boiling, then 1% sodium citrate aqueous solution (2 mL) was added slowly. The solution was kept boiling for 1 hour to produce GO-Ag nanocomposites. Then, the product was washed with DI water three times.

The content of silver in AgNPs and GO-Ag nanocomposites were measured using inductively coupled plasma atomic emission spectroscopy (ICP-AES). Concentrations of GO and GO-Ag were measured using spectrometer and weighing method after lyophilization. Absorption spectrum of GO, AgNP and GO-Ag were recorded using spectrophotometer. GO and GO-Ag were also characterized by transmission electron microscopy (TEM; Tecnai G20 F20, FEI).

Photothermal heating curves were recorded by infrared thermal camera. AgNP, GO and GO-Ag were added into LB broth with volume ratio of 1:9, and final concentrations of them were 4 μg mL<sup>-1</sup>, 3 μg mL<sup>-1</sup> and 7

$\mu\text{g mL}^{-1}$  respectively. 1 mL LB broth contained different nanomaterial as well as DI water as control were added into 24-well plate, solution was irradiated continuously by NIR laser light ( $808\text{ nm}$ ,  $1.5\text{ W cm}^{-2}$ ) for 7 minutes at room temperature.

## **MIC determination of antibacterial agents against MDR *E. coli***

According to a reported protocol [49], agar dilution method was used for MIC determination. At first, LB agar contained different concentrations of antimicrobials were prepared, and then  $2\ \mu\text{L}$  bacteria ( $10,000\text{ CFU}$ ) were dropped on surface of the agar. The inoculum was allowed to be absorbed into the agar for 0.5 hour before 16 hours incubation in  $37\text{ }^{\circ}\text{C}$  incubator. Susceptibility of 2 MDR bacteria strains to a serial concentration of antibacterial agents were tested at least three times. Tested materials were GO-Ag, AgNPs, AMP, TET, STR and CHL, corresponding concentrations were 0, 2, 4, 8, 16, 32, 64, 128, 256,  $512\ \mu\text{g mL}^{-1}$ .

## ***In vitro* antibacterial assessment of different antibacterial agents**

Single colony on agar plate was transferred to fresh LB broth, and then cultured for 12 to 16 hours in  $37\text{ }^{\circ}\text{C}$  shaker at speed of 250 rotations per minute. The cultured bacteria were collected, and supernatant was removed after centrifugation. Bacteria pellet was resuspended in 4.5 mL fresh LB broth to a final concentration of  $10^7\text{--}10^8\text{ CFU mL}^{-1}$ . Then, 0.5 mL nanomaterials of different concentrations were added into broth and mixed well. The broth was then incubated with nanomaterials at  $37\text{ }^{\circ}\text{C}$  for 3 hours before viability assessment. Tested antibacterial agents included GO, AgNPs, GO-Ag, GO+AgNPs (mixture of GO and AgNPs), corresponding components concentrations of GO were  $1.5\ \mu\text{g mL}^{-1}$ ,  $3\ \mu\text{g mL}^{-1}$ ,  $6\ \mu\text{g mL}^{-1}$ , and silver were  $2\ \mu\text{g mL}^{-1}$ ,  $4\ \mu\text{g mL}^{-1}$ ,  $8\ \mu\text{g mL}^{-1}$ . 3 replicate samples were tested for each treated group.

Similar with reported protocol evaluated interaction between biomaterial and cell [50], MTT assay was used to evaluate bacterial viability after antimicrobial agents incubation. 0.1 mL bacteria culture was transferred into 96 well plate, and then mixed well with  $20\ \mu\text{L}$  5 mg/mL MTT solution for 16 hours' culture in  $37\text{ }^{\circ}\text{C}$  incubator. After centrifugation for 5 minutes at 2000 RPM, supernatant was removed from microplate and replaced with  $120\ \mu\text{L}$  DMSO in each well, then microplate was shaken for 10 minutes to dissolve precipitants. At last, recording  $\text{OD}_{570}$  with microplate reader (Bio-Rad). All the samples were replicated for 3 times.

## ***In vitro* photothermal treatment of MDR-2 *E. coli***

Overnight cultured MDR-2 bacteria were collected and resuspended in fresh LB broth to a final concentration of  $10^7$ – $10^8$  CFU mL<sup>-1</sup>. Then, 10% volume of nanocomposites (GO, GO-Ag) or water (control) was added into LB broth, final concentration of GO and GO-Ag were 3  $\mu\text{g mL}^{-1}$  and 7  $\mu\text{g mL}^{-1}$ . The broth was shaken at 37 °C for 1 hour before laser irradiation. 1 mL bacteria culture was transferred into one well of 24-well plate, 808 nm laser light was used to irradiate the broth. Irradiation lasted for 7 minutes at different energy density, including 0, 1.0, 1.5 and 2.0 W cm<sup>-2</sup>. Temperature during laser irradiation was indicated by thermal camera. After irradiation, the mixture was cultured for 6 hours before bacteria viability assessment. Viability assessment was conducted by spread plate method and MTT assay.

## Fluorescent imaging of treated MDR-2 *E. coli*

With or without photothermal irradiation (1.5 W cm<sup>-2</sup>, 7 minutes) and 7  $\mu\text{g mL}^{-1}$  GO-Ag treatment, MDR-2 *E. coli* were cultured for 6 hours before collection. Collected bacteria cells were washed and stained with 4'-6-diamidino-2-phenylindole (DAPI) and propidium iodide (PI) according to reported protocol [51]. Bacteria were washed in 10 mM MgSO<sub>4</sub> at pH 6.5 after centrifugation and then stained with PI (5  $\mu\text{g mL}^{-1}$ ) and DAPI (5  $\mu\text{g mL}^{-1}$ ) for 30 minutes in dark. After dried in air, the samples were observed under confocal microscope (Leica TCS SP5 II).

## Morphology characterization of MDR-2 *E. coli*

MDR-2 *E. coli* treated with or without 14  $\mu\text{g mL}^{-1}$  GO-Ag were cultured in LB broth for 3 hours, and then bacteria were collected and washed three times with PBS buffer. After fixed with 2.5% glutaraldehyde solution, the cells were dehydrated by sequential treatment of 50%, 70%, 90% and 100% ethanol for 15 minutes. With gold sputter-coating, bacteria were imaged with scanning electron microscope (SEM, Quanta 200FEG, FEI).

## Results

### Antibacterial agents' characterization

In this study, GO, AgNP and GO-Ag were synthesized to investigate their antibacterial efficiency. Following reported protocol, GO sheets were prepared at first. As Figure 1a showed, thin GO sheet was synthesized successfully. Afterwards, AgNPs were grown on GO sheets by in situ reducing silver nitrate solution on surface of GO sheet. The synthesized GO-Ag nanocomposite was confirmed by observed absorption band around 440 nm (Figure 1c) and TEM image (Figure 1b).

NIR photothermal heating curve of GO-Ag, GO, AgNP and LB broth were recorded by thermal camera. In Figure 1d, GO-Ag showed better photothermal efficiency than AgNP and GO. Temperature increasement of

control, AgNP, GO and GO-Ag were 13.6 °C, 12 °C, 18.9 °C and 24.6 °C after 7 minutes irradiation.

## MIC comparison testing using agar dilution method

MIC is defined as the lowest concentration of an antimicrobial that inhibits visible growth of a microorganism after overnight incubation. MIC of AgNP, GO-Ag and three types of antibiotics (penicillin, tetracycline and aminoglycoside) against 2 clinical MDR bacteria strains were tested by agar dilution method. Test results showed that these 2 bacteria were resistant to AMP, TET and STR or CHL. MIC values of all the typical antibiotics were  $\geq 256 \mu\text{g mL}^{-1}$ . While for the nanomaterial-based antibacterial agents, the dose was much lower. As shown in Table 1, MIC of GO-Ag and AgNPs were  $4 \mu\text{g mL}^{-1}$  and  $32 \mu\text{g mL}^{-1}$  respectively. Compared with AgNP, a widely used antimicrobial agent, GO-Ag showed much higher antibacterial efficiency against 2 clinical MDR *E. coli* stains. Growth of MDR-1 and MDR-2 bacteria on LB agar could be inhibited with  $4 \mu\text{g mL}^{-1}$  GO-Ag. No visual colony was observed on surface of agar even 10,000 CFU bacteria were cultured on agar media overnight.

## Synergetic antibacterial effect verification of GO-Ag

In order to find why GO-Ag nanocomposites showed higher antibacterial efficiency than AgNPs, we decomposed GO-Ag nanocomposites and measured the ratio of GO and Ag by ICP and weighing method. Results showed content of GO and AgNP were 57% and 43% respectively in GO-Ag nanocomposite. Afterwards, antibacterial efficiency of GO-Ag, AgNP, GO, and mixture of GO and AgNP (denoted as GO+AgNP) were studied in LB broth. Three concentrations nanomaterials were tested, corresponding concentrations of AgNP were 2, 4, 8  $\mu\text{g mL}^{-1}$ , and GO were 1.5, 3, 6  $\mu\text{g mL}^{-1}$ . Incubation time of 3 hours was selected as bacteria was in the middle of log phase, which made it easy to discriminate minor difference between treated and control groups.

MTT assay results in Figure 2 indicated that GO-Ag owning the highest antibacterial efficiency among tested nanomaterials. As concentration increased, GO-Ag showed efficient antibacterial effect against 2 MDR *E. coli*. Remained viabilities of MDR-1 and MDR-2 were 77.1%, 52.2%, 4.4% and 88.9%, 66.8%, 4.1% respectively, corresponding to increasing concentrations of 3.5  $\mu\text{g mL}^{-1}$ , 7  $\mu\text{g mL}^{-1}$ , 14  $\mu\text{g mL}^{-1}$ . While there was no obvious decrease trend of remained bacteria viability with increased concentration of GO or AgNP. In AgNP treated group, the remained viability of MDR-1 and MDR-2 were in the range of 81.8%–99.1%, when AgNP concentration ranged from 2  $\mu\text{g mL}^{-1}$  to 8  $\mu\text{g mL}^{-1}$ . In GO treated group, the remained viability of MDR-1 and MDR-2 were in the ranges of 87.7% to 95.1% and 99.3% to 105.9%, when GO concentrations increased from 1.5  $\mu\text{g mL}^{-1}$  to 6  $\mu\text{g mL}^{-1}$ . Compared with GO-Ag nanocomposite, GO+AgNP mixture did not show observable viability decrease trend with increasing mixture concentration. The above results demonstrated that higher antibacterial efficiency of GO-Ag nanocomposites arose from synergetic effect of GO and AgNPs when the two materials are combined as composite. Moreover, 2 MDR *E. coli* bacteria showed similar response to different nanomaterial. A minor

difference was that MDR-2 bacteria was less susceptible to GO-Ag at lower concentrations ( $3.5 \mu\text{g mL}^{-1}$ ,  $7 \mu\text{g mL}^{-1}$ ), when compared with MDR-1 bacteria.

## ***In vitro* photothermal-assisted treatment of MDR-2**

As a matter of fact, GO-Ag owned property of converting electromagnetic energy to heat, which might elevate its antibacterial efficiency. As shown in Figure 1d, GO-Ag nanocomposites converted electromagnetic energy to heat more efficiently than GO sheets and AgNPs. Temperature increment of GO-Ag nanocomposites group was approximately  $25 \text{ }^\circ\text{C}$  after 7 minutes irradiation.

Photothermal treatment of MDR-2 *E. coli* using GO-Ag nanocomposites was conducted. MDR-2 was selected as it was non-susceptible to more antibiotics and less susceptible to GO-Ag at lower concentrations.  $10^7$ – $10^8$  CFU  $\text{mL}^{-1}$  bacteria were cultured with  $7 \mu\text{g mL}^{-1}$  GO-Ag nanocomposites or  $3 \mu\text{g mL}^{-1}$  GO in LB broth for 1 hour. Afterwards, 808 nm NIR laser irradiation was exerted continuously on bacteria culture for 7 minutes, as illustrated in Figure 3a. At last, the bacteria culture was collected for cell viability assessment using MTT assay and spread plate method. Data obtained from two methods were consistent with each other, as shown in Figure 3b and Figure 3c. In this study, incubation time of 6 hours was used because bacteria in control group was in plateau phase. As a result, we could figure out whether bacteria growth was stopped completely after photothermal treatment. In control group without antibacterial agents, different power density laser irradiation, ranging from  $1.0$  to  $2.0 \text{ W cm}^{-2}$ , had no observable inhibitory effect against MDR-2 *E. coli*. Compared with GO sheets, GO-Ag was more efficient to resist the growth of bacteria. Bacteria viability was 3.0% in GO-Ag treated group with  $1.5 \text{ W cm}^{-2}$  power density exerted, while 94.7% in GO sheets treated group under the same condition. When power density was increased to  $2 \text{ W cm}^{-2}$ , MDR-2 *E. coli* could be killed completely in GO-Ag treated group. However, without photothermal treatment in GO-Ag group, the remained viability was 69%. Thus, efficient antibacterial effect could be achieved with use of GO-Ag at lower concentrations when photothermal treatment was exerted simultaneously.

## **Characterization of GO-Ag treated MDR bacteria**

The above results demonstrated that GO-Ag nanocomposites were highly effective antibacterial agent, but whether bacteria growth was inhibited temporarily or permanently remained unclear. Fluorescent imaging was used to distinguish living and non-living bacteria (red color in Figure 4). Photothermal irradiation and GO-Ag treatment were 2 variants that influence bacteria viability. Fluorescent imaging was conducted to observe changes of bacteria living status that induced by 2 variants. As shown in Figure 4, 4 groups of bacteria were imaged under confocal microscope. In the two control groups without GO-Ag nanocomposites addition (GO-Ag -), the number of dead cells was very less as they were in log-phase, and the laser irradiation did not induce bacteria death. In contrast, the group with GO-Ag nanocomposites addition and without laser irradiation (GO-Ag +, laser -), almost all the bacteria were dead. Moreover,

antibacterial efficiency of GO-Ag was enhanced when laser irradiation and GO-Ag treatment were combined. In the group with GO-Ag nanocomposites addition and laser irradiation (GO-Ag +, laser +), fewer cells could be found in the visual in comparison with group without laser irradiation (GO-Ag +, laser -). Results indicated that both GO-Ag treatment and photothermal treatment could result in non-living bacteria.

Furthermore, morphology of MDR-2 bacteria were characterized using SEM after treatment with  $14 \mu\text{g mL}^{-1}$  GO-Ag nanocomposites. As shown by arrows in Figure 5, some pits were found on the surface of cell wall, which meant cell walls were disrupted after GO-Ag nanocomposites treatment. While in the control group, cell wall was smooth and no cell integrity disruption was observed.

## Discussion

It was reported GO-Ag could not only inhibit growth of non-susceptible bacteria, including Gram-positive *S. aureus* and Gram-negative *E. coli* [38, 52], but also inhibit growth of Methicillin-resistant *S. aureus* [39] and fungus like *Candida albicans* and *Candida tropicalis* [42]. In this work, clinical isolated MDR *E. coli* were selected as samples to test the antibacterial efficiency of GO-Ag nanocomposites *in-vitro*. It was proved GO-Ag nanocomposites was effective against MDR *E. coli*, which broaden its antimicrobial spectrum. Moreover, the most important advance was photothermal treatment was combined for the first time in GO-Ag antibacterial applications.

GO-Ag nanocomposites showed antibacterial effect in both liquid and solid medium (Table 1, Figure 2). As MIC results showed,  $4 \mu\text{g mL}^{-1}$  GO-Ag could completely inhibit growth of  $10^4$  CFU bacteria on agar plate. In broth, ratio of survival bacteria was  $< 5\%$  when  $14 \mu\text{g mL}^{-1}$  GO-Ag was added into  $10^7$ – $10^8$  CFU/mL bacteria culture. AgNPs also showed antibacterial effect, but efficiency was not so obvious. MIC of AgNP was  $32 \mu\text{g mL}^{-1}$  on agar medium. While  $8 \mu\text{g mL}^{-1}$  AgNP addition in broth had minor antibacterial effect to 2 MDR bacteria. GO treated bacteria, showed no viability decrease trend with increased concentration from  $1.5 \mu\text{g mL}^{-1}$  to  $6 \mu\text{g mL}^{-1}$ , though several published papers reported that GO was an antimicrobial agent. The different antibacterial property of GO might come from difference of material preparation method, dose, material size, culturing condition and sample handling method [53–58].

Higher antibacterial efficiency of GO-Ag nanocomposites can be explained by that: AgNPs were well distributed on GO sheets, which provided large contact area between bacteria and AgNPs. Compared with GO, AgNPs and mixture of GO and AgNPs, GO-Ag nanocomposite treated group achieved better antibacterial result at same concentration of Ag or GO, which disclosed existence of synergetic effect that arose from combining GO and AgNPs as composite. And this synergetic effect was consistent with previous reported works [38, 39].

Compared with other reported GO-Ag related antimicrobial applications, photothermal therapy was combined in this study for the first time. An important benefit was that GO-Ag dose could be cut down,

which was an advantage for biomedical applications.  $7 \mu\text{g mL}^{-1}$  GO-Ag could completely killed bacteria in photothermal combined therapy, while  $14 \mu\text{g mL}^{-1}$  GO-Ag could not completely inhibited MDR bacteria growth. Photothermal-assistant therapy could greatly enhance antibacterial efficiency as GO-Ag possessed advantages of AgNP and GO. AgNP inhibited bacteria growth, while GO sheets absorbed the NIR light and generated heat to help killing bacteria. Another advantage of photothermal therapy was that it could kill MDR bacteria even if bacteria were resistant to GO-Ag. Thus, photothermal-assistant therapy with GO-Ag provides an alternative strategy to solve problems bring by drug-resistant bacteria.

In order to better understand interaction between GO-Ag nanocomposites and bacteria, fluorescent images (Figure 4) and SEM images of treated *E. coli* were analyzed (Figure 5). Fluorescent imaging was used to distinguish living and dead bacteria using optimized PI staining process for bacteria [51]. DAPI was used to stain DNA-containing bacteria regardless of their physiological status, while PI was used to stain membrane-compromised bacteria [59–61]. In fluorescent images, red-light fluorescence emitted from GO-Ag and photothermal treated groups, demonstrated that both GO-Ag nanocomposites and photothermal treatment could damage bacteria integrity. Morphology characterization confirmed that cell integrity was disrupted by GO-Ag nanocomposites, which was consistent with published results[38, 39] [52].

This study provided a facial method to synthesize GO-Ag nanocomposite, which possessed synergetic antibacterial property as well as photothermal property. It provided double insurance to combat traditional antibiotics resistant bacteria, and achieved consensus enhanced antibacterial efficiency to pathogens. Given the excellent antibacterial performance of GO-Ag nanocomposites to widely distributed MDR *E. coli* bacteria, it will be a useful antimicrobial in the future medical applications. For example, GO-Ag nanocomposites can be coated onto consumables such as bandage, gauze and woundplast, or surgical devices such as lancet, surgical scissors and surgical suture that have chances to contact with infection bacteria.

## Conclusions

Compared with widely used AgNP, GO-Ag nanocomposite showed much better antibacterial efficiency to clinical isolated MDR *E. coli*. Moreover, photothermal treatment could be combined to further lowering dose to  $7 \mu\text{g mL}^{-1}$  to completely kill MDR *E. coli*. Fluorescent imaging and morphology characterization disclosed that bacteria integrity was damaged after treatment with GO-Ag. Given the excellent antibacterial performance of GO-Ag nanocomposites against widely distributed MDR *E. coli* bacteria, it could be useful antibacterial consumables in the future medical applications.

## Abbreviations

GO, graphene oxide; AgNPs, silver nanoparticles; GO-Ag, graphene oxide-silver nanoparticles nanocomposite; SEM, scanning electron microscope; TEM, transmission electron microscope; NIR, near-infrared; ICP-AES, inductively coupled plasma atomic emission spectroscopy;

MIC, minimum inhibitory concentration; *E. coli*, *Escherichia coli*; *S. aureus*, *Staphylococcus aureus*; LB, Luria-Bertani; DI, distilled; MDR, multidrug-resistant; XDR, extensively drug-resistant; PDR, pandrug-resistant; DNA, deoxyribonucleic acid; ENT, ear, nose and throat;

DAPI, 4'-6-diamidino-2-phenylindole; PI, propidium iodide; CFU, colony forming unit; AMP, ampicillin; TET, tetracycline; NAL, nalidixic acid; STR, streptomycin; SPE, spectinomycin; GEN, gentamicin; CHL, chloramphenicol; DMSO, dimethyl sulfoxide; MTT, thiazolyl blue tetrazolium bromide;

µg, microgram; mL, milliliter;

## **Declarations**

## **Ethics approval and consent to participate**

Not applicable.

## **Consent for publication**

Not applicable.

## **Availability of data and materials**

All data generated or analysed during this study are included in this published article.

## **Competing Interests**

The authors declare that they have no competing interests.

## **Funding**

This work is supported by “Young Project of Wuxi Health and Family Planning Commission Q201809”.

## **Authors' contributions**

Chen Yuqing and Wu Wei contributed equally to this work. All authors read and approved the final manuscript.

## **Acknowledgements**

Not applicable.

## References

1. Czaplewski L, Bax R, Clokie M, Dawson M, Fairhead H, Fischetti VA, Foster S, Gilmore BF, Hancock REW, Harper D *et al*: *Alternatives to antibiotics-a pipeline portfolio review. Lancet Infectious Diseases* 2016, *16*(2):239–251.
2. Tenover FCJTAjom: *Mechanisms of antimicrobial resistance in bacteria. The American Journal of Medicine* 2006, *119*(6):S3-S10.
3. Magiorakos AP, Srinivasan A, Carey RB, Carmeli Y, Falagas ME, Giske CG, Harbarth S, Hindler JF, Kahlmeter G, Olsson-Liljequist B *et al*: *Multidrug-resistant, extensively drug-resistant and pandrug-resistant bacteria: an international expert proposal for interim standard definitions for acquired resistance. Clinical Microbiology and Infection* 2012, *18*(3):268–281.
4. Nseir S, Di Pompeo C, Cavestri B, Jozefowicz E, Nyunga M, Soubrier S, Roussel-Delvallez M, Saulnier F, Mathieu D, Durocher A: *Multiple-drug-resistant bacteria in patients with severe acute exacerbation of chronic obstructive pulmonary disease: Prevalence, risk factors, and outcome. Critical Care Medicine* 2006, *34*(12):2959–2966.
5. Herati RS, Blumberg EA: *Losing ground: multidrug-resistant bacteria in solid-organ transplantation. Current Opinion in Infectious Diseases* 2012, *25*(4):445–449.
6. Tatarelli P, Mikulska M: *Multidrug-resistant bacteria in hematology patients: emerging threats. Future Microbiology* 2016, *11*(6):767–780.
7. Flores-Mireles AL, Walker JN, Caparon M, Hultgren SJ: *Urinary tract infections: epidemiology, mechanisms of infection and treatment options. Nat Rev Microbiol* 2015, *13*(5):269–284.
8. Manges AR, Johnson JR, Foxman B, O'Bryan TT, Fullerton KE, Riley LW: *Widespread distribution of urinary tract infections caused by a multidrug-resistant Escherichia coli clonal group. The New England journal of medicine* 2001, *345*(14):1007–1013.
9. Linton A, HOWE K, Bennett P, Richmond M, Whiteside EJJoAB: *The colonization of the human gut by antibiotic resistant Escherichia coli from chickens. Journal of Applied Bacteriology* 1977, *43*(3):465–469.
10. Sáenz Y, Brinas L, Domínguez E, Ruiz J, Zarazaga M, Vila J, Torres CJAA, chemotherapy: *Mechanisms of resistance in multiple-antibiotic-resistant Escherichia coli strains of human, animal, and food origins. Antimicrobial agents and chemotherapy* 2004, *48*(10):3996–4001.
11. Meng J, Zhao S, Doyle MP, Joseph SW: *Antibiotic resistance of Escherichia coli O157:H7 and O157:NM isolated from animals, food, and humans. Journal of food protection* 1998, *61*(11):1511–1514.

12. Bensink JC, Bothmann FP: *Antibiotic-resistant Escherichia coli isolated from chilled meat at retail outlets. New Zealand veterinary journal* 1991, 39(4):126–128.
13. Johnson JR, Kuskowski MA, Smith K, O'Bryan TT, Tatini S, Joid: *Antimicrobial-resistant and extraintestinal pathogenic Escherichia coli in retail foods. The Journal of infectious diseases* 2005, 191(7):1040–1049.
14. Watkinson A, Micalizzi G, Graham G, Bates J, Costanzo S, JAEM: *Antibiotic-resistant Escherichia coli in wastewaters, surface waters, and oysters from an urban riverine system. Appl Environ Microbiol* 2007, 73(17):5667–5670.
15. Forsberg KJ, Reyes A, Wang B, Selleck EM, Sommer MO, Dantas GJs: *The shared antibiotic resistome of soil bacteria and human pathogens. science* 2012, 337(6098):1107–1111.
16. Seil JT, Webster TJ: *Antimicrobial applications of nanotechnology: methods and literature. International Journal of Nanomedicine* 2012, 7:2767–2781.
17. Sirelkhatim A, Mahmud S, Seeni A, Kaus NHM, Ann LC, Bakhori SKM, Hasan H, Mohamad D: *Review on Zinc Oxide Nanoparticles: Antibacterial Activity and Toxicity Mechanism. Nano-Micro Letters* 2015, 7(3):219–242.
18. Fu GF, Vary PS, Lin CT: *Anatase TiO<sub>2</sub> nanocomposites for antimicrobial coatings. Journal of Physical Chemistry B* 2005, 109(18):8889–8898.
19. Dizaj SM, Lotfipour F, Barzegar-Jalali M, Zarrintan MH, Adibkia K: *Antimicrobial activity of the metals and metal oxide nanoparticles. Materials Science & Engineering C-Materials for Biological Applications* 2014, 44:278–284.
20. Sharma VK, Yngard RA, Lin Y: *Silver nanoparticles: Green synthesis and their antimicrobial activities. Advances in Colloid and Interface Science* 2009, 145(1–2):83–96.
21. Rai MK, Deshmukh SD, Ingle AP, Gade AK: *Silver nanoparticles: the powerful nanoweapon against multidrug-resistant bacteria. Journal of Applied Microbiology* 2012, 112(5):841–852.
22. Taylor PL, Ussher AL, Burrell RE: *Impact of heat on nanocrystalline silver dressings Part I: Chemical and biological properties. Biomaterials* 2005, 26(35):7221–7229.
23. Guzman M, Dille J, Godet S: *Synthesis and antibacterial activity of silver nanoparticles against gram-positive and gram-negative bacteria. Nanomedicine-Nanotechnology Biology and Medicine* 2012, 8(1):37–45.
24. Thomas R, Nair AP, Soumya KR, Mathew J, Radhakrishnan EK: *Antibacterial Activity and Synergistic Effect of Biosynthesized AgNPs with Antibiotics Against Multidrug-Resistant Biofilm-Forming Coagulase-*

- Negative Staphylococci Isolated from Clinical Samples. Applied Biochemistry and Biotechnology* 2014, 173(2):449–460.
- 25.Radzig MA, Nadtochenko VA, Koksharova OA, Kiwi J, Lipasova VA, Khmel IA: *Antibacterial effects of silver nanoparticles on gram-negative bacteria: Influence on the growth and biofilms formation, mechanisms of action. Colloids and Surfaces B-Biointerfaces* 2013, 102:300–306.
- 26.Chen M, Yu X, Huo Q, Yuan Q, Li X, Xu C, Bao H: *Biomedical Potentialities of Silver Nanoparticles for Clinical Multiple Drug-Resistant Acinetobacter baumannii. Journal of Nanomaterials* 2019.
- 27.Geim AK, Novoselov KS: *The rise of graphene. Nature Materials* 2007, 6(3):183–191.
- 28.Geim AK: *Graphene: Status and Prospects. Science* 2009, 324(5934):1530–1534.
- 29.Zhu YW, Murali S, Cai WW, Li XS, Suk JW, Potts JR, Ruoff RS: *Graphene and Graphene Oxide: Synthesis, Properties, and Applications. Advanced Materials* 2010, 22(35):3906–3924.
- 30.Ji H, Sun H, Qu X: *Antibacterial applications of graphene-based nanomaterials: Recent achievements and challenges. Advanced Drug Delivery Reviews* 2016, 105:176–189.
- 31.Markovic ZM, Jovanovic SP, Maskovic PZ, Danko M, Micusik M, Pavlovic VB, Milivojevic DD, Kleinova A, Spitalsky Z, Markovic BMT: *Photo-induced antibacterial activity of four graphene based nanomaterials on a wide range of bacteria. Rsc Advances* 2018, 8(55):31337–31347.
- 32.Luo Y, Yang X, Tan X, Xu L, Liu Z, Xiao J, Peng R: *Functionalized graphene oxide in microbial engineering: An effective stimulator for bacterial growth. Carbon* 2016, 103:172–180.
- 33.Ruiz ON, Fernando KAS, Wang BJ, Brown NA, Luo PG, McNamara ND, Vangsness M, Sun YP, Bunker CE: *Graphene Oxide: A Nonspecific Enhancer of Cellular Growth. Acs Nano* 2011, 5(10):8100–8107.
- 34.Fiocca K, Normil N, Ellison M, Lobo A: *Antibiotic delivery in resistant Escherichia coli using PEG-modified nano-graphene oxide. Abstracts of Papers of the American Chemical Society* 2016, 251.
- 35.Xiao L, Sun J, Liu L, Hu R, Lu H, Cheng C, Huang Y, Wang S, Geng J: *Enhanced Photothermal Bactericidal Activity of the Reduced Graphene Oxide Modified by Cationic Water-Soluble Conjugated Polymer. Acs Applied Materials & Interfaces* 2017, 9(6):5382–5391.
- 36.Wu M-C, Deokar AR, Liao J-H, Shih P-Y, Ling Y-C: *Graphene-Based Photothermal Agent for Rapid and Effective Killing of Bacteria. Acs Nano* 2013, 7(2):1281–1290.
- 37.Jaworski S, Wierzbicki M, Sawosz E, Jung A, Gielerak G, Biernat J, Jaremek H, Lojkowski W, Wozniak B, Wojnarowicz J et al: *Graphene Oxide-Based Nanocomposites Decorated with Silver Nanoparticles as an Antibacterial Agent. Nanoscale Research Letters* 2018, 13.

38. Tang J, Chen Q, Xu L, Zhang S, Feng L, Cheng L, Xu H, Liu Z, Peng R: *Graphene Oxide-Silver Nanocomposite As a Highly Effective Antibacterial Agent with Species-Specific Mechanisms. Acs Applied Materials & Interfaces* 2013, 5(9):3867–3874.
39. Mazarin de Moraes AC, Lima BA, de Faria AF, Brocchi M, Alves OL: *Graphene oxide-silver nanocomposite as a promising biocidal agent against methicillin-resistant Staphylococcus aureus. International Journal of Nanomedicine* 2015, 10:6847–6861.
40. Xu W-P, Zhang L-C, Li J-P, Lu Y, Li H-H, Ma Y-N, Wang W-D, Yu S-H: *Facile synthesis of silver@graphene oxide nanocomposites and their enhanced antibacterial properties. Journal of Materials Chemistry* 2011, 21(12):4593–4597.
41. Prasad K, Lekshmi GS, Ostrikov K, Lussini V, Blinco J, Mohandas M, Vasilev K, Bottle S, Bazaka K, Ostrikov K: *Synergic bactericidal effects of reduced graphene oxide and silver nanoparticles against Gram-positive and Gram-negative bacteria. Scientific Reports* 2017, 7.
42. Li C, Wang X, Chen F, Zhang C, Zhi X, Wang K, Cui D: *The antifungal activity of graphene oxide-silver nanocomposites. Biomaterials* 2013, 34(15):3882–3890.
43. Tian T, Shi X, Cheng L, Luo Y, Dong Z, Gong H, Xu L, Zhong Z, Peng R, Liu Z: *Graphene-Based Nanocomposite As an Effective, Multifunctional, and Recyclable Antibacterial Agent. Acs Applied Materials & Interfaces* 2014, 6(11):8542–8548.
44. Hendry AT, Stewart IO: *Silver-resistant Enterobacteriaceae from hospital patients. Canadian journal of microbiology* 1979, 25(8):915–921.
45. Finley PJ, Norton R, Austin C, Mitchell A, Zank S, Durham P: *Unprecedented Silver Resistance in Clinically Isolated Enterobacteriaceae: Major Implications for Burn and Wound Management. Antimicrobial Agents and Chemotherapy* 2015, 59(8):4734–4741.
46. Lee P, Meisel DJTJoPC: *Adsorption and surface-enhanced Raman of dyes on silver and gold sols. The Journal of Physical Chemistry* 1982, 86(17):3391–3395.
47. Sun X, Liu Z, Welsher K, Robinson JT, Goodwin A, Zaric S, Dai HJNr: *Nano-graphene oxide for cellular imaging and drug delivery. Nano research* 2008, 1(3):203–212.
48. Hummers Jr WS, Offeman REJJoTacs: *Preparation of graphitic oxide. Journal of the american chemical society* 1958, 80(6):1339–1339.
49. Andrews JMJJoaC: *Determination of minimum inhibitory concentrations. Journal of antimicrobial Chemotherapy* 2001, 48(suppl\_1):5–16.
50. Ciapetti G, Cenni E, Pratelli L, Pizzoferrato A: *INVITRO EVALUATION OF CELL BIOMATERIAL INTERACTION BY MTT ASSAY. Biomaterials* 1993, 14(5):359–364.

51. Williams S, Hong Y, Danavall D, Howard-Jones M, Gibson D, Frischer M, Verity PJJoMM: *Distinguishing between living and nonliving bacteria: evaluation of the vital stain propidium iodide and its combined use with molecular probes in aquatic samples. Journal of Microbiological Methods* 1998, 32(3):225–236.
52. Ma J, Zhang J, Xiong Z, Yong Y, Zhao XS: *Preparation, characterization and antibacterial properties of silver-modified graphene oxide. Journal of Materials Chemistry* 2011, 21(10):3350–3352.
53. Akhavan O, Ghaderi E: *Toxicity of Graphene and Graphene Oxide Nanowalls Against Bacteria. Acs Nano* 2010, 4(10):5731–5736.
54. Liu S, Zeng TH, Hofmann M, Burcombe E, Wei J, Jiang R, Kong J, Chen Y: *Antibacterial Activity of Graphite, Graphite Oxide, Graphene Oxide, and Reduced Graphene Oxide: Membrane and Oxidative Stress. Acs Nano* 2011, 5(9):6971–6980.
55. He JL, Zhu XD, Qi ZN, Wang C, Mao XJ, Zhu CL, He ZY, Lo MY, Tang ZS: *Killing Dental Pathogens Using Antibacterial Graphene Oxide. Acs Applied Materials & Interfaces* 2015, 7(9):5605–5611.
56. Chen J, Peng H, Wang X, Shao F, Yuan Z, Han H: *Graphene oxide exhibits broad-spectrum antimicrobial activity against bacterial phytopathogens and fungal conidia by intertwining and membrane perturbation. Nanoscale* 2014, 6(3):1879–1889.
57. Perreault F, de Faria AF, Nejati S, Elimelech M: *Antimicrobial Properties of Graphene Oxide Nanosheets: Why Size Matters. Acs Nano* 2015, 9(7):7226–7236.
58. Yousefi M, Dadashpour M, Hejazi M, Hasanzadeh M, Behnam B, de la Guardia M, Shadjou N, Mokhtarzadeh A: *Anti-bacterial activity of graphene oxide as a new weapon nanomaterial to combat multidrug-resistance bacteria. Materials Science & Engineering C-Materials for Biological Applications* 2017, 74:568–581.
59. Jepras RI, Carter J, Pearson SC, Paul FE, Wilkinson MJ: *DEVELOPMENT OF A ROBUST FLOW CYTOMETRIC ASSAY FOR DETERMINING NUMBERS OF VIABLE BACTERIA. Applied and Environmental Microbiology* 1995, 61(7):2696–2701.
60. Lopezamoros R, Comas J, Vivesrego J: *FLOW CYTOMETRIC ASSESSMENT OF ESCHERICHIA-COLI AND SALMONELLA-TYPHIMURIUM STARVATION-SURVIVAL IN SEAWATER USING RHODAMINE-123, PROPIDIUM IODIDE, AND OXONOL. Applied and Environmental Microbiology* 1995, 61(7):2521–2526.
61. Sgorbati S, Barbesti S, Citterio S, Bestetti G, DeVecchi R: *Characterization of number, DNA content, viability and cell size of bacteria from natural environments using DAPI/PI dual staining and flow cytometry. Minerva Biotechnol* 1996, 8(1):9–15.

## Table

**Table 1.** MICs of MDR *E. coli*

	GO-Ag ( $\mu\text{g mL}^{-1}$ )	AgNP ( $\mu\text{g mL}^{-1}$ )	AMP ( $\mu\text{g mL}^{-1}$ )	STR/CHL ( $\mu\text{g mL}^{-1}$ )	TET ( $\mu\text{g mL}^{-1}$ )
MDR-1*	4	32	>512	>512 (Str)	256
MDR-2*	4	32	>512	>512 (Chl)	512

\*MDR-1 and MDR-2 were two isolates of MDR *E. coli* from clinical samples. MDR-1 was resistant to ampicillin (AMP), tetracycline (TET), nalidixic acid (NAL) and streptomycin (STR), MDR-2 was resistant to ampicillin (AMP), tetracycline (TET), nalidixic acid (NAL) and chloramphenicol (CHL), spectinomycin (SPE) and gentamicin (GEN).

## Figures

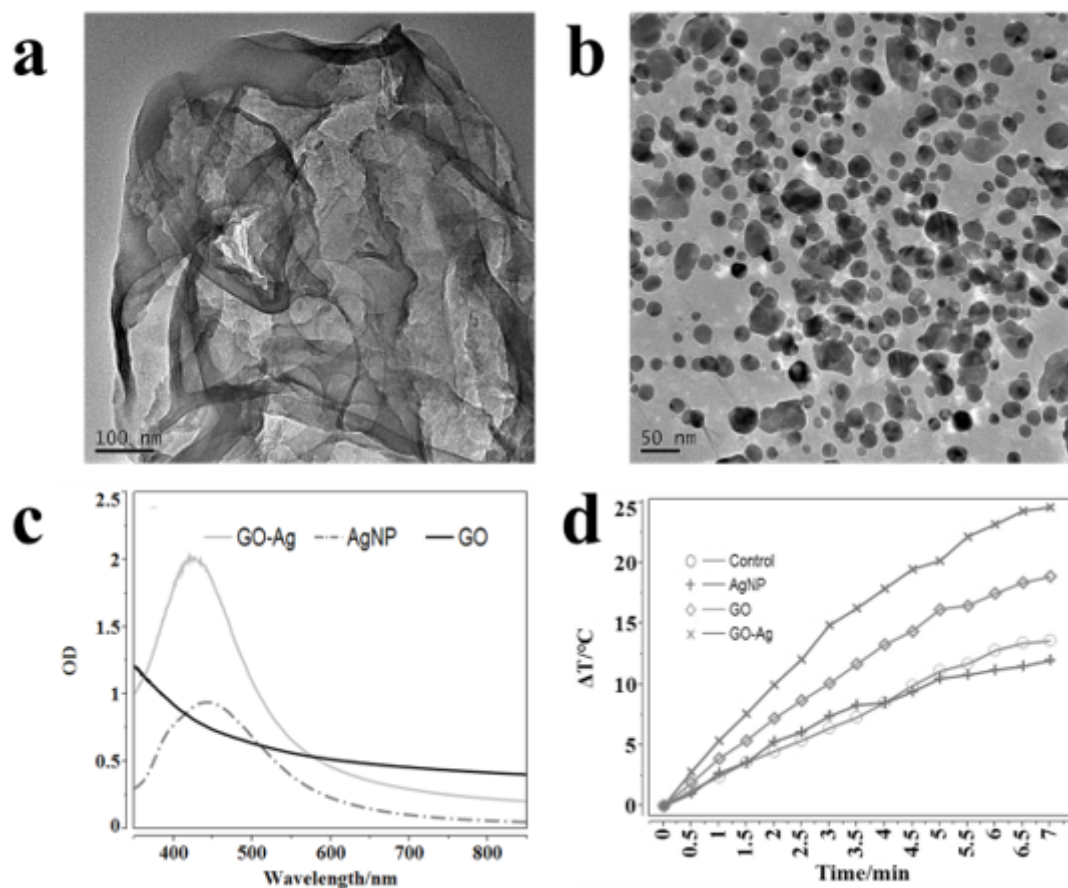


**Figure 1**

Characterization of synthesized nanomaterials. (a) TEM image of graphene oxide (GO). (b) TEM image of graphene oxide-silver (GO-Ag) nanocomposites. (c) Absorption spectrum of GO, AgNP and GO-Ag. (d) Photothermal heating curves of AgNP, GO, GO-Ag and LB broth (control) under 808 nm laser irradiation, the concentrations of AgNP, GO, GO-Ag were 4  $\mu\text{g mL}^{-1}$ , 3  $\mu\text{g mL}^{-1}$ , 7  $\mu\text{g mL}^{-1}$  respectively.

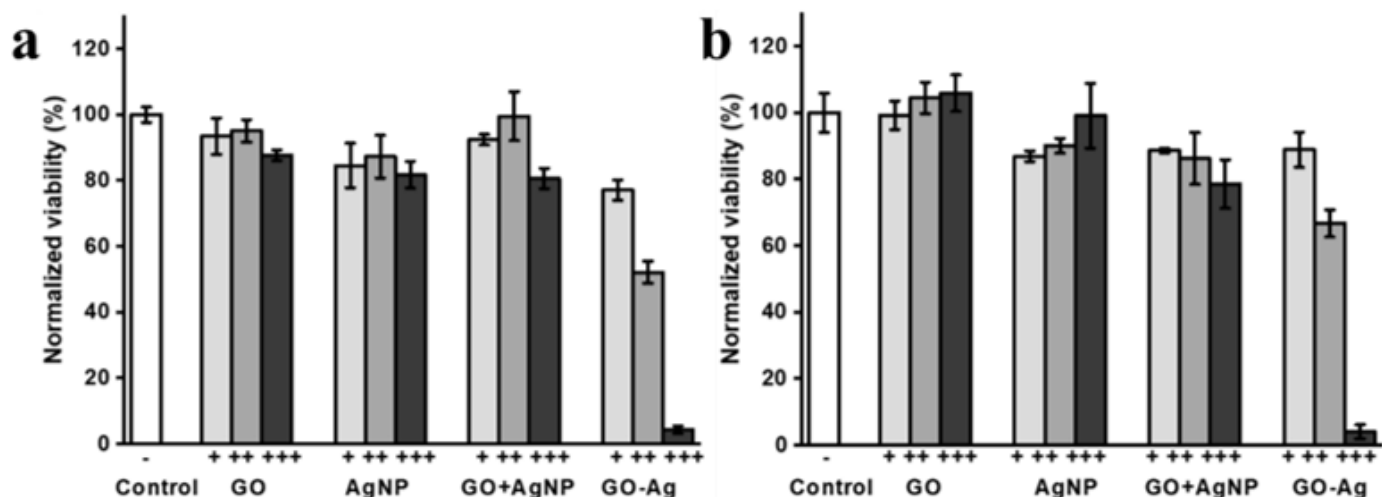


**Figure 2**

MDR E. coli viability assessment by MTT assay. (a) MDR-1 E. coli viability and (b) MDR-2 E. coli viability after treatment with GO, AgNP, GO-Ag, mixture of GO and AgNP at different final concentrations in LB liquid broth. Symbol +, ++, +++ represent different concentrations for different nanomaterial groups. GO (+, 1.5  $\mu\text{g mL}^{-1}$ ; ++, 3  $\mu\text{g mL}^{-1}$ ; +++, 6  $\mu\text{g mL}^{-1}$ ), AgNP (+, 2  $\mu\text{g mL}^{-1}$ ; ++, 4  $\mu\text{g mL}^{-1}$ ; +++, 8  $\mu\text{g mL}^{-1}$ ), GO+AgNP mixture (+, 1.5  $\mu\text{g mL}^{-1}$  GO and 2  $\mu\text{g mL}^{-1}$  AgNP; ++, 3  $\mu\text{g mL}^{-1}$  GO and 4  $\mu\text{g mL}^{-1}$  AgNP; +++, 6  $\mu\text{g mL}^{-1}$  GO and 8  $\mu\text{g mL}^{-1}$  AgNP), GO-Ag (+, 3.5  $\mu\text{g mL}^{-1}$ ; ++, 7  $\mu\text{g mL}^{-1}$ ; +++, 14  $\mu\text{g mL}^{-1}$ ). Error bars represent standard deviations.

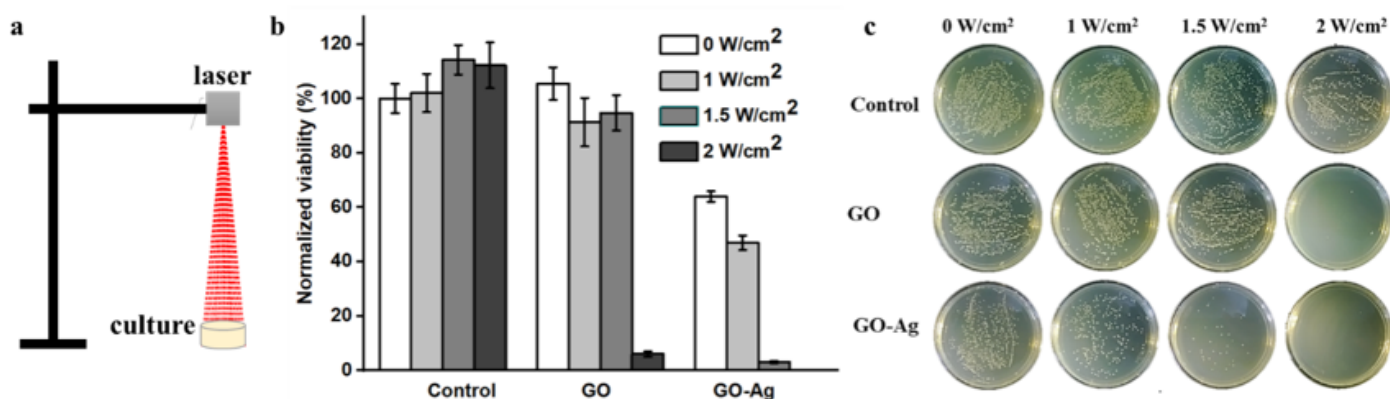


**Figure 3**

In vitro photothermal treatment of MDR-2 E. coli. (a) Illustration of photothermal treatment of bacteria in LB broth. (b) Bacteria viability results using MTT assay after photothermal treatment at different power density for 7 minutes. (c) Photos of bacteria colonies on LB agar plates after photothermal treatment at different power density for 7 minutes. Error bars represent standard deviations ( $n \geq 3$ ).

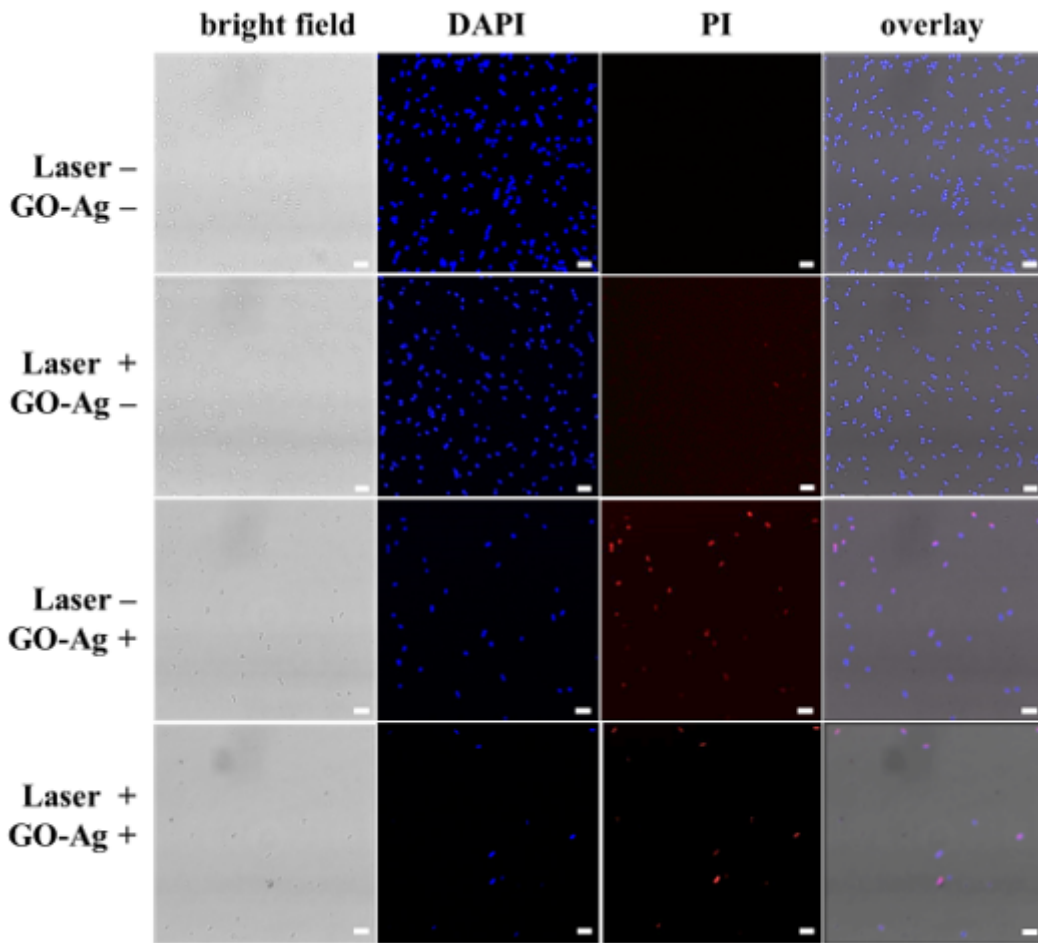


**Figure 4**

Fluorescent imaging of MDR-2 *E. coli* with and without photothermal-assisted treatment. DAPI and PI were used to stain the nuclei acid of bacteria. The difference is DAPI stains all the bacteria while PI can only stain the non-living bacteria. DAPI stained bacteria emit blue fluorescent light while PI stained bacteria emit red fluorescent light. Symbol "Laser +" and "Laser -" denote with and without photothermal treatment respectively, "GO-Ag +" and "GO-Ag -" denote with and without GO-Ag nanocomposites treatment respectively. Power density was 1.5 W cm<sup>-2</sup> and GO-Ag concentration was 7 µg mL<sup>-1</sup>. Scale bar is 5 µm.

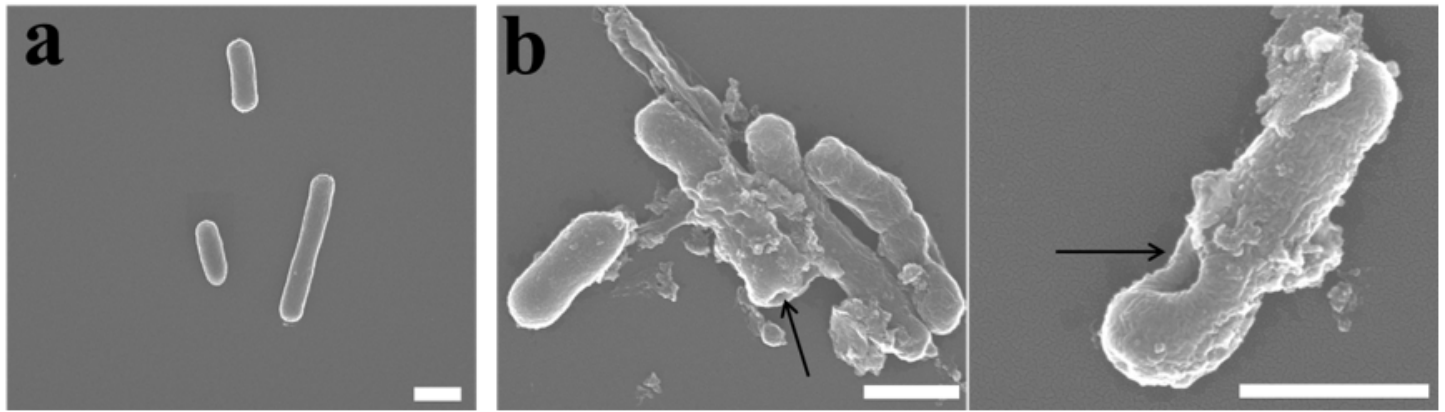


**Figure 5**

SEM images of MDR-2 *E. coli*. (a) SEM image of control group without GO-Ag treatment. (b) SEM images of bacteria treated with  $14 \mu\text{g mL}^{-1}$  GO-Ag. Arrows show disrupted cell wall. Scale bar is  $1 \mu\text{m}$ .